Journal of Environmental Management 344 (2023) 118476

Contents lists available at ScienceDirect

Journal of Environmental Management

journal homepage: www.elsevier.com/locate/jenvman

Research article

MgO-mediated activation of active carbon as an affordable strategy to "in situ" degradation of lindane in contaminated soils

Javier Erro [a,*], José-Manuel Martínez-Pérez [a], Maitane Guembe Contreras [b], Raúl López Márquez [c], José María García-Mina [a]

[a] Environmental Biology Department, Faculty of Sciences, BIOMA Institute, University of Navarra, C/Irunlarrea, 1, 31008, Pamplona, Spain
[b] Magnesitas Navarra, S.A, Av. Roncesvalles, 31630, Zubiri, Navarra, Spain
[c] Emgrisa S.A, Santiago Rusiñol, 12, 28040, Madrid, Spain

ARTICLE INFO

Keywords:
Soil remediation
Heavy metals
Dehydrohalogenation
Dihaloelimination
Adsorption

ABSTRACT

The accumulation in soil landfills of toxic and persistent lindane, widely used as an insecticide, triggers the risk of leaching with the concomitant contamination of surrounding rivers. Thus, viable remediation to eliminate in situ high concentrations of lindane in soil and water becomes an urgent demand. In this line, a simple and cost-effective composite is proposed, including the use of industrial wastes. It includes reductive and non-reductive base-catalyzed strategies to remove lindane in the media. A mixture of magnesium oxide (MgO) and activated carbon (AC) was selected for that purpose. The use of MgO provides a basic pH. In addition, the specific selected MgO forms double-layered hydroxides in water which permits the total adsorption of the main heavy metals in contaminated soils. AC provides adsorption microsites to hold the lindane and a reductive atmosphere that was increased when combined with the MgO. These properties trigger highly efficient remediation of the composite. It permits a complete elimination of lindane in the solution. In soils doped with lindane and heavy metals, it produces a rapid, complete, and stable elimination of lindane and immobilization of the metals. Finally, the composite tested in lindane-highly contaminated soils permits the "in situ" degradation of nearly 70% of the initial lindane. The proposed strategy opens a promising way to face this environmental issue with a simple, cost-effective composite to degrade lindane and fix heavy metals in contaminated soils.

1. Introduction

Lindane, the γ-isomer of hexachlorocyclohexane (HCH), is a broad-spectrum insecticide with very high efficacy that has been widely used in agriculture worldwide in recent decades (Vijgen et al., 2011). Lindane is highly toxic to humans and animals and harms ecological ecosystems (Dorsey, 2005). In addition, the degradation of lindane in the soil, either by the action of native microorganisms or by natural chemical agents, is very slow, thus causing its considerable permanence in the soil. For all these reasons, lindane has been banned in many developed countries (Madaj et al., 2018). However, many soil areas in the countries where lindane was manufactured and stored are highly contaminated by lindane residues (Fernández et al., 2013). This is the case of Sabiñanigo in Spain (longitude: 0°20′45.38"; latitude: 42°30′52"; altitude: 783 m), where the accumulation of lindane and lindane metabolites in some soil areas can reach up to 1000 mg kg^{-1}, with an average of 300–400 mg kg^{-1}. This situation is found in many other countries where lindane was produced and was confined once its use was banned. In this critical environmental problem, the development of feasible approaches for the in situ remediation of lindane-contaminated soils is particularly relevant.

Some studies have reported on the efficiency of soil bioremediation techniques using specific microorganisms to degrade lindane in soils (Kumar and Pannu, 2018). However, these technologies are adequate for low concentrations of lindane in the soil due to its high toxicity, which affects the survival of microorganisms (Zhang, W. et al., 2014, 2020; Kumar and Pannu, 2018). On the other hand, many studies have shown that lindane can be readily degraded in aquatic environments using two complementary remediation pathways involving elimination reactions. The elimination reactions may be reductive and non-reductive (Li et al., 2011). The non-reductive elimination is also called β-elimination or dehydrohalogenation and consists of the loss of chloride and adjacent proton to form a C=C double bond. The main byproducts formed are 1, 2, 4-Trichlorobencene (TCB), 1, 3, 5-TCB and 1, 2, 3-TCB

* Corresponding author.
E-mail address: jerrogar@unav.es (J. Erro).

https://doi.org/10.1016/j.jenvman.2023.118476
Received 29 March 2023; Received in revised form 6 June 2023; Accepted 19 June 2023
Available online 4 July 2023

(Li et al., 2011). It is catalyzed by hydroxide. In this line, in situ chemical oxidation (ISCO) techniques use peroxide and persulfate activated by organic compounds as activated carbon, quinones or humic acids as they can act as electron mediators (Usman et al., 2014, 2017; Aguinaco, A. et al., 2011; Ma et al., 2018). The reductive elimination can involve two processes: dihaloelimination and hydrogenolysis in an acidic medium (Li et al., 2011). A characteristic byproduct of the reductive dihaloelimination is 1, 2-Dichorobencene (DCB).

However, these methodologies, which are very efficient to eliminate lindane in water or soil-water suspensions, are not feasible to be used directly in the soil for in situ remediation. In this context, our work describes a new cost-effective composite that can degrade lindane directly in soil for in situ remediation by combining basic-catalyzed dehydrohalogenation and reductive dihaloelimination. Our working hypothesis is that we could use these two complementary pathways for lindane degradation through the interaction of lindane with a particular composite endowed with microsites with a high capacity for lindane uptake, a reducing atmosphere, and a strongly basic local pH. We have explored the combination of strong basic materials (metal oxides and hydroxides) and absorbent organic materials such as biochar or activated carbon to obtain this material. After some preliminary studies, among the different potential materials, we have found that the most profitable combination was magnesium oxide and activated carbon. An additional advantage of this combination is that magnesium oxide has a high capacity to immobilize heavy metals in soils, thus preventing their mobility and eventual transfer to groundwater (García et al., 2004). In addition, the selected magnesium oxide could form layered double hydroxides (LDH) with high sorption efficiency (Tang, Z. et al., 2020). In this line, Zhang et al. (2015) joined magnetite, graphene and LDH, Pramanik et al. (2018), Aldawsari, A. M. et al. (2021), Al Juboury, M. F. and Abdul-Hameed, H. M. (2020) combined the LDH with activated carbon and Vithanage, M. et al. (2020) and Zubair, M. et al. (2021) joined LDH with biochar However, all the studies were oriented to water media. In this way, we have a multipurpose decontaminating composite capable of simultaneously treating in situ lindane and other organic contaminants and heavy metals in soils.

The main objectives of this study involves (i) the synthesis of a composite following the mentioned strategy, (ii) the characterization of the proposed composite at a structural, computational and mechanistic level, (iii) the study in vitro of its efficiency in solution, and (iv) the study in real conditions of its efficiency in field and in doped soils.

2. Material and methods

2.1. Synthesis of the composite

The composite (ACP) includes a specific magnesium oxide (MgO), PC8, obtained from the production of MgO-based products in Magnesitas Navarra S.A. It constitutes a byproduct, and its inclusion is part of a circular strategy involved in ACP design and production. This type of MgO was selected according to its granulometry (Table S1) and its high ability to immobilize heavy metals compared with other MgO-based products and byproducts (Supplementary Information, Annex 1. Fig. S1). The selected MgO (PC8) was mixed using a conventional powder mixer with powdered activated carbon purchased from Merck. Powder mixing was made at 23 °C and atmospheric pressure for 1 h. The organic absorbing material, active carbon (AC) was selected among different samples, including two biochars and active carbon. The main property for selecting the material was its ability to remove phenol from a water solution. Phenol was selected as a model organic contaminant because of its balance between polarity and hydrophobicity. The study is described in Supplementary Information, Annex 2 (Fig. S2). Different proportions of activated carbon (AC) were tested following the economic and technical criteria described in Supplementary Information, Annex 3 (Fig. S3).

2.2. Physicochemical characterization of ACP

2.2.1. X-ray diffraction analysis

The mineralogical phases contained in PC8, activated carbon, and in ACP -before and after treating with pollutants-were analyzed and compared by X-ray diffraction (XRD) using a Bruker D8 Advance diffractometer (Karlsruhe, Germany), according to the diffraction powder method, with a CuKα1 radiation and 0.02° 2θ increment and 1s·step^{-1} sweep from 2° to 90° 2θ. The results were compared with the ICDD database.

2.2.2. SEM-EDX

The samples were finely ground, and a portion of the sample was placed on an SEM sample stub. The samples were scanned in a Philips model XL30FEG-SEM scanning electron microscope (accelerating voltage of 15 kV) using an EDAX Phoenix energy disperse spectroscopy analyzer (EDX).

Following the exploratory analysis, samples were scanned for specific structures with defined micromorphology. The scanning procedure consisted of analyzing by EDX for qualitative elemental composition a selected area which was also photographed at 5000x and 200,00x.

2.2.3. FTIR

Functional group distribution in ACP structure and its components (PC8 and AC) were characterized using ATR-FTIR spectroscopy. Attenuated Total Reflectance (ATR) infrared spectra were recorded over the 4000-600 cm^{-1} range with a resolution of 4 cm^{-1} in a Shimadzu IRAffinity-1-S.

2.2.4. Pore size and surface area

An ASAP 2020 adsorption device (Micrometrics GmbH, Moenchengladbach, Germany) was used to determine the specific surface area, specific pore volume, and pore sizes of PC8 before and after hydrating. Specific surfaces areas were obtained using the multipoint Brunauer–Emmet–Teller (BET) method. The corresponding specific pore volume and pore sizes were determined using the Horvath-Kawazoe (HK) methods.

2.2.5. Reducing capacity of ACP

Solutions of three doses of ACP and solutions of each of the components separately (100, 500, and 1000 ppm of activated carbon; and 600, 3000, and 6000 ppm of PC8) were prepared in $K_3Fe(CN)_6$ 0.25 mM, previously dissolved in a borate buffer. After 24 h in dark conditions, absorbance was determined at 420 nm by UV–vis spectroscopy. The reducing power of the tested materials was expressed as electron transfer capacity, according to Xin et al. (2018).

2.2.6. Molecular modeling

Theoretical calculations were performed with Gaussian 16 W, and normal modes were analyzed in Gauss View 6.0. Geometry optimization followed by frequency calculations was performed based on the density functional theory (DFT) method at the APF-D/6-311G (2 d, p) level of theory.

2.3. In vitro essays of ACP efficiency

2.3.1. Degradation of lindane in solution

Solutions of 6 ppm of lindane in water were prepared to test the lindane removal efficiency of ACP. Two doses of activated carbon (AC and ACx2: 250 and 500 ppm), 250 ppm AC basified with NaOH, 3000 ppm of PC8, and ACP1 (250 ppm AC + 3000 ppm PC8) were tested in 200 mL of lindane solution in glass bottles. Samples were stirred in dark conditions for seven days, and the supernatant samples were used to determine the remaining lindane in the solution. The solid residue corresponding to each treatment was isolated by centrifugation (2000 g, 2 min) and treated with 200 ml n-hexane 1 h to desorb the lindane

present in the solid. Both adsorbed and water remaining lindane were determined by gas chromatography/mass spectrometry (GC/MS) in CNTA accredited laboratory (Centro Nacional de Tecnología y Seguridad Alimentaria., Spain) to analyze lindane and metabolites in soil, plants and foods. The method used is based on US EPA 8270D (Semivolatile organic compounds by gas chromatography/Mass Spectrometry). A dispersive liquid–liquid microextraction method was applied for the trace determination of organochlorine pesticides. In the same way, the main degradation products were measured: volatile organic compounds, organochlorine pesticides and phenols. Samples corresponded to a pool of 3 individual samples per treatment.

2.3.2. Lindane degradation and heavy metal fixation in soil

An alkaline soil with low available P was doped with 500 ppm of lindane and 1000 ppm of heavy metals (Cu, Mn, Ni, Zn, Cd, As and Pb). To this end, an aqueous solution with the heavy metals and another solution of lindane dissolved in hexane, were prepared and added to the soil. Different ACP at 15% were mixed with the soil, and the mixture was watered to field capacity:

ACP 1: activated carbon 7% + PC8 93%

ACP 2: activated carbon 14% + PC8 86%

A control without ACP was kept to compare the efficiency of the treatments. Three samples per treatment were taken each week from 24 h to 50 days from treating in order to have three replicates. Organic pollutants were extracted to determine lindane and byproducts by gas chromatography/mass spectrometry (GC/MS) following the QuEChERS method for pesticide residues (Vera et al., 2013). The analysis was made in Agrupalab accredited laboratory (Derio, Spain) using a method based on US EPA 8270D (Semivolatile organic compounds by gas chromatography/Mass Spectrometry).

Heavy metals were extracted with water and determined by ICP-OES. Briefly, three samples were taken from each treatment, and 20 g were dissolved in 40 mL of water and shaken in a Heidolph reax 2 model mixer overhead at the medium speed for 30 min. Finally, samples were centrifuged (4500 g, 20 min) and the supernatant were analyzed by ICP-OES.

2.4. Lindane degradation in a highly contaminated soil

A field assay was carried out in Bailín (Sabiñánigo). In this region of Spain, there are dump sites of lindane in landfills. The samples contained around 500 ppm of the sum of all the isomers of hexachlorocyclohexane. The applied doses of each treatment were 15% in soil (15 g ACP/100 g soil), and the composition of each ACP was the following:

ACP 1: activated carbon 7% + PC8 93%

ACP 2: activated carbon 14% + PC8 86%

A control of the soil without any treatment was also prepared.

The study area was 10 m^3 of the landfill to have a representative field surface. In this context, preliminary studies demonstrated that the heterogeneous distribution of the particulate lindane impairs obtaining homogenous samples (data not shown). Therefore studies were carried out to obtain representing samples by selecting the most homogeneous areas of the dump, followed by cryogenic grinding of representative soil samples. In that way, several samples of 5 kg of mud from that place were taken and treated with ACP. Samples of the mud were air-dried, mixed with each treatment, and watered to field capacity, and samples at 7, 14, 28, and 50 days from the beginning were taken. Hexachlorocyclohexanes from each sample were extracted and products and byproducts were determined in the Agrupalab laboratory accredited laboratory as described above.

3. Results and discussion

3.1. Description of ACP

The MgO material was selected from different sources provided by Magnesitas Navarras SA. They included marketed products and some byproducts. Apart from economic viability, the two main properties considered for MgO selection were the pH in solution and the ability to immobilize the following heavy metals. The study carried out to select MgO-based product is described in Supplementary Information, Annex 1 (Fig. S1).

The most efficient product was the byproduct named PC8 (Fig. S1). It is produced during the process of magnesium carbonate calcination to produce MgO and is recovered in the cyclone filters used for air purification. Its mineral composition comprises 63.92% of MgO, 6.43% of CaO, 5.16% of SiO_3, and 2.50% of Fe_2O_3. As shown in Fig. 1a, the different phases included in this material are magnesite, calcite, dolomite, anhydrite, and periclase (Ismailov et al., 2020). Regarding its grain size, 98.48% is under 200 μm, with 84% under 45 μm. The small particle size and the presence of trivalent cations, especially iron, could explain the high adsorption capacity of this material. Oxides that include di and trivalent cations in their structure can form in contact with water layered double hydroxides (LDH) with the following form: $[M^{2+}_{1-x}\ N^{3+}_{x}\ (OH)_2]^{x+}\ [(X^{n-})_{x/n} \cdot yH_2O]^{x-}$. These oxyhydroxides are characterized by their high adsorption capacity (Gao et al., 2018; Manohara et al., 2011; Tang et al., 2020). This fact differentiated this compound from the rest of magnesium oxides making it more efficient to remove heavy metals from the media. Fig. 1b, c, d show the XRD and SEM-EDX micrographs of PC8 after treated with a water solution containing the heavy metals. The three peaks that characterize the presence of local LDH can be observed (Gao et al., 2018; Zhang et al., 2015). However, their intensity is low because their presence is restricted where Fe is accumulated. LDH are observed in the SEM-EDX micrographs of Fig. 1c and d (Tao et al., 2006) along with the accumulation of heavy metals. Finally, the presence of LDH in the hydrated PC8 was also suggested in the increase of surface area and in the slit pore geometry observed for hydrated PC8 related to anhydrous PC8 (Fig. 2).

The 1H, and 13C-NMR of AC were not possible due to its magnetization in the rotor, which impairs the rotation of the sample. Fig. 3a and b shows the XRD and SEM micrograph of AC. The XRD pattern showed the activated carbon in semi-crystalline form, which is indicated by the broad peaks (002) and (100) at the 2θ around 25° and 45°, which can be attributed to the amorphous carbon and graphite structure, respectively. The narrow reflections are related to the presence of quartz as an impurity (Keppetipola et al., 2021). This presence of silicates with sorption capacity could enhance the adsorption property of the AC. SEM image of AC displays the porosity structure with cavities that would act as local sites for pollutants sorption (Keppetipola et al., 2021).

Two AC/PC8 (ACP) combinations were considered for the studies:

ACP1: 7% AC + 93% PC8.

ACP2: 14% AC + 86% PC8.

These formulations are obtained by conventional mixing, as described in detail in Methods.

These two compositions were selected after evaluating the efficiency of the individual components and ACP to eliminate lindane from a water solution, as described below.

3.2. Efficiency of ACP to eliminate lindane in solution

ACP and its components were tested for lindane removal from the solution.

Two doses of activated carbon (AC and ACx2: 250 and 500 ppm), 250 ppm AC basified with NaOH, 3000 ppm of PC8, and ACP1 (250 ppm AC + 3000 ppm PC8) were tested in 200 mL of lindane solution in glass bottles.

Solutions of 6 ppm of lindane in water were prepared to test the lindane removal efficiency of ACP. The methodology is described in detail in Methods.

To assess whether the removal of lindane is associated with its absorption into the material and its subsequent degradation, we treated the solid materials with hexane to analyze the proportion of lindane that is

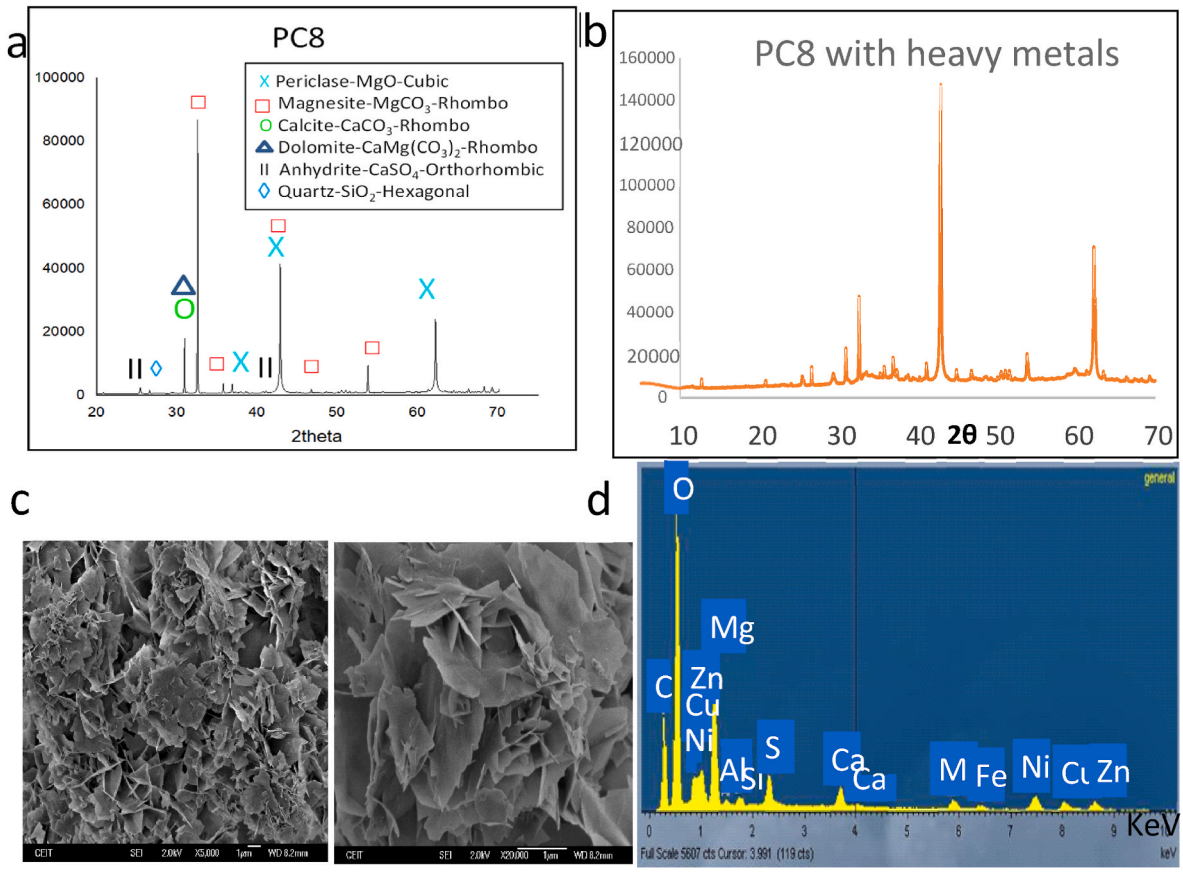

Fig. 1. MgO PC8 characterization and interaction with heavy metals in solution. **a.** XRD of MgO PC8 **b.** XRD of MgO PC8 after mixing in solution with heavy metals (Ni, Cu, Zn, Mn), appearance of LDH-like peaks. **c.** SEM of MgO PC8 after mixing in solution with heavy metals, presence of LDH-like structures. **d.** EDX of MgO PC8 in the solution with heavy metals, presence of the metals in the MgO.

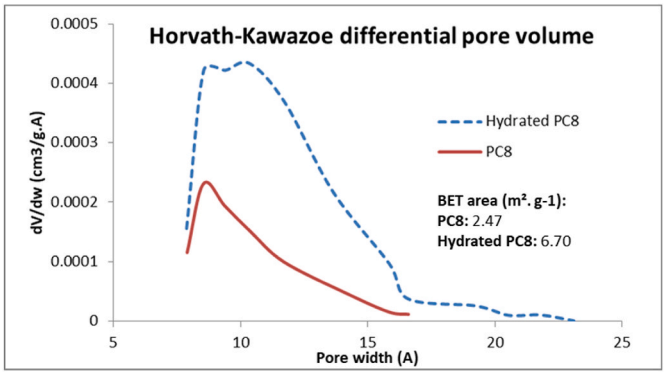

Fig. 2. PC8 and hydrated PC8 pore and surface area analysis.

absorbed but not degraded. Fig. 4a shows the ability of PC8 and AC to remove lindane from the solution. The two doses of AC, and PC8 removed 100% of the lindane in the solution. PC8 desorbed 47.8% and AC 63.4% of the previously adsorbed lindane (Fig. 4a). By doubling the AC dose, there was an increase in the clearance of lindane, reaching the 33.8% of lindane removed, but far from 100% of the lindane present in the media. These results clearly show the sorption capacity of both PC8 and AC. The results agree well with the adsorption capacity of the LDH formed in PC8 and the reported capacity of AC to absorb organic molecules (Liu et al., 2017). In that way, the SEM image of ACP1 reflects the presence of the LDH structures in ACP (Tao et al., 2006) as well as a homogeneous and regular form of the ACP1 (Fig. 4b). The partial degradation of lindane with AC suggests a reducing capacity of AC besides its sorption capacity (Fu et al., 1993; Kirisits et al., 2000; Li et al., 2010; Ruowen et al., 1993). These results were also reflected in the presence of chloride in EDX analysis of AC samples after treatment of lindane solution (Fig. 4c). Likewise, FTIR spectra of PC8 in solution, apart from support the formation of LDH(peak of OH at 3700 cm^{-1}, Fig. 3d and e) (Tao et al., 2006), shows the formation of $MgCl_2$ (https://www.chemicalbook.com/SpectrumEN_7786-30-3_ir1.htm) observed in the presence of lindane in solution (peak at 2800-3000 cm^{-1}) which also reflects lindane elimination by PC8 (Fig. 4f). This conclusion is supported by the presence of 1, 2-DCB, which is mainly associated with the reductive dihaloelimination process, as will be discussed later (Table 1) (Li et al., 2011). Likewise, this is in line with the reducing power of PC8 and, specially, of AC observed in the ferricyanide test, where the reducing capacity of the ACP and its components was evaluated (Fig. 5a).

Lindane is completely removed when AC is added and the pH is basified with NaOH (Fig. 4a).

On the other hand, when ACP1 was tested and PC8 and AC worked together, there was a complete elimination (absorption and degradation) of the lindane presented in the media (Fig. 4a). This result clearly shows the synergetic action of PC8 and AC when working simultaneously.

To study the type of elimination pathway involved in the degradation of lindane by ACP, the analysis of the main byproducts derived from the reaction of lindane with ACP1 and its components, both in solution and in solid materials, was carried out (Table 1). The presence of chlorides in the solution when applying PC8 and the ACP indicates the dechlorination of lindane, releasing chloride into the medium. In the case of treatment with AC, chlorides are also observed but adsorbed on AC (Table 1). This is in line with SEM-EDX images of Fig. 4c. In the same

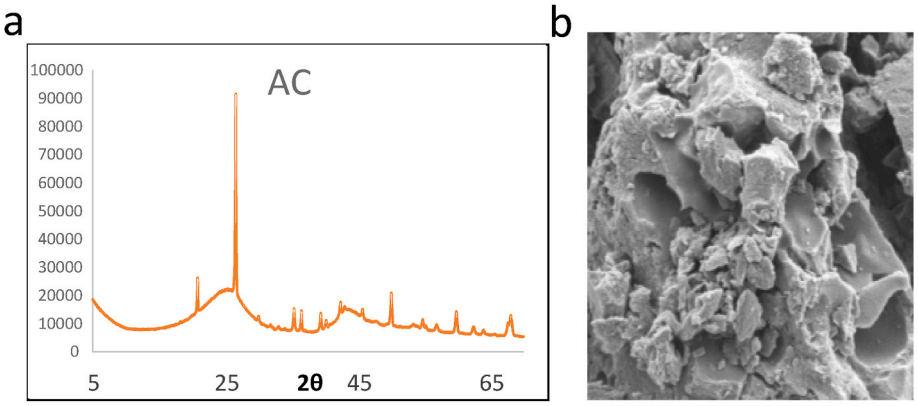

Fig. 3. AC characterization. **a.** XRD of AC. **b.** SEM of AC.

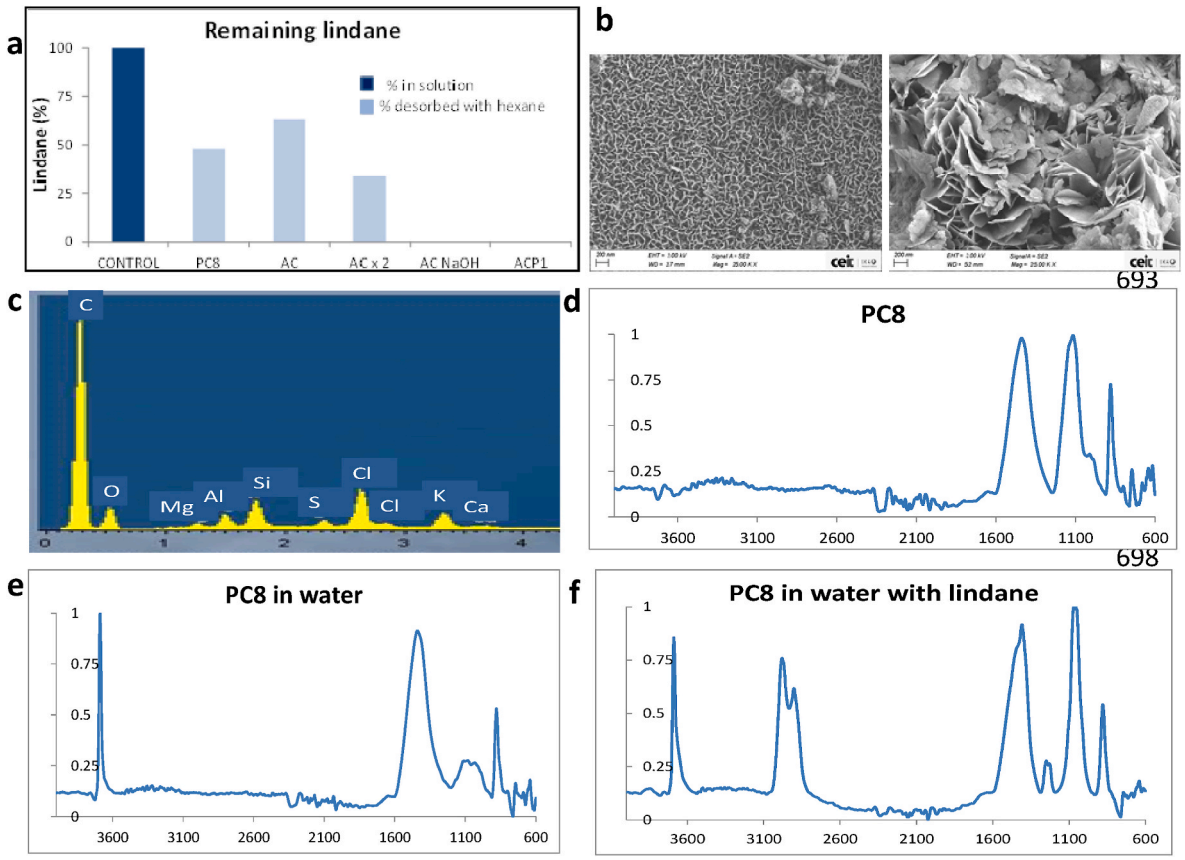

Fig. 4. Interaction of ACP and its compounds with lindane in solution **a.** Lindane remaining in solution and desorbed from components of ACP after treating with them **b.** SEM of ACP in solution with lindane **c.** EDX of the AC in solution with lindane, presence of Cl in AC **d.** FTIR spectra of PC8, **e.** PC8 in water and **f.** PC8 in aqueous solution of lindane.

way, part of the chlorides is also fixed to PC8 and ACP1. This fact underlies the dechlorination capacity of AC, PC8, and ACP1 and their capacity to fix the byproducts resulting from the degradation of lindane. The other main byproduct observed in the solution and fixed in PC8 and ACP1 is 1, 2, 4-TCB. It is also detected by treating the lindane solution with AC plus NaOH. This product has been reported as the main byproduct obtained from lindane-elimination through base-catalyzed dehydrohalogenation, indicating that this process is associated with lindane degradation by these treatments (Li et al., 2011). This is consistent with the highly basic pH associated with PC8 and NaOH. Finally, 1, 2-DCB is also detected in PC8 and, especially, in ACP1. This byproduct has been linked to the reductive mechanism of dihaloelimination, indicating that this reductive pathway is also involved in eliminating lindane by these treatments (Li et al., 2011). This result is in line with the previously observed reducing property of ACP1, which is directly related to the combination of PC8 and AC (Fig. 5a).

These results indicate that ACP1 can remove lindane with an effect resulting from the synergistic interaction of its two components: On the one hand, the fixation of lindane in AC in the presence of the hydroxide produced by the hydrolysis of PC8 favors the development of basic-catalyzed dehydrohalogenation; on the other hand, the PC8 activation of the reducing power of AC favors the reduction of lindane by dihaloelimination.

Table 1
Byproducts remaining in solution after treatments (A); and byproducts remaining in the solid residue after treatments (B).

A. Byproducts remaining in solution (μg kg^{-1} dry basis)

	CONTROL	AC	PC8	ACP1	NaOH 1 N
Chlorides	<2000	<5000	7020	7210	<5000
1,2,4-Trichlorobenzene	<5	<5	>60 (113)	<5	>60 (87.6)

B. Byproducts remaining in the solid (mg kg-1 dry basis)

	AC	PC8	ACP1
Chlorides (1:5 p/v)	105,000	24,900	22,300
1,2,4-Trichlorobenzene	<0.3	1.08	1.13
1,2-Dichlorobenzene	<0.3	0.112	0.76
α-Hexachlorociclohexane	0.921	<0.2	<0.2

3.3. Lindane electronic-molecular distribution implications in its interaction with ACP

The highly hydrophobic character of lindane suggests that the hydrophobic effect mainly governs its interaction with AC Carbon matrix. However, the presence of chlorine atoms in the structure and their high electronegativity can drive a particular electronic distribution with local sites with positive- and negative-partial charges. These local sites, in turn, can favor the presence of electrostatic interactions between lindane and the AC surface. In addition, induced polarization also plays a significant role in the potential of these sites. In that way, the chlorine orientation in lindane, with three equatorial and three highly reactive axial (non-coplanar) substituents, generates a big dipole moment that could affect the electrostatic configuration of local sites. Some studies have shown the usefulness of molecular electrostatic potential (MEP) calculations in explaining the role of non-covalent electrostatic interactions in the mechanism underlying specific chemical reactions (Murray and Politzer, 2017). In the case of lindane, the halogen atoms can affect the distribution of electronic density in the different regions of the molecule and, thereby, the electrostatic potential at the molecular surface and the space surrounding the molecule. The heterogeneous distribution of electronic density is usually, but not always, associated with concomitant MEP changes that induce the formation of local sites with positive electrostatic potential called σ and π-holes. These local MEP sites, in particular, can drive chemical bonding. We hypothesize that the possible presence of local σ/π holes in the lindane structure could also be involved in the binding of lindane to AC and PC8. To explore this hypothesis, the electronic density and MEP distribution of lindane were calculated using the APF-D hybrid DFT method using the basis set 6-31G (2 d,p). Several studies have shown that this basis set used with DFT produces reliable MEP distributions (Murray and Politzer, 2017).

Fig. 5b and c shows the optimized structure of lindane (γ-isomer of HCH) and the MEP distribution on the molecular surface. The results clearly show a large molecule area with positive electrostatic potential corresponding to some of the protons adjacent to the chlorine atoms. This area likely drives hydroxide attack, leading to the loss of the chlorine and the adjacent proton, forming a C═C double bond. However, the presence of σ holes in the chlorine atoms should be noted. These σ holes could be involved in the interaction of lindane with the negative-charged sites (aromatic π electrons or oxygen-containing groups, such as carboxylic or phenolic acids) in the AC structure. These results are compatible with non-covalent electrostatic interactions in the binding of lindane in AC.

3.4. Efficiency of ACP to eliminate lindane and immobilize heavy metals in a modified soil at laboratory level

To investigate the ability of ACP formulations to remove lindane and immobilize heavy metals in soil, contaminated soil, artificially doped with lindane and heavy metals, was prepared. This approach allowed for

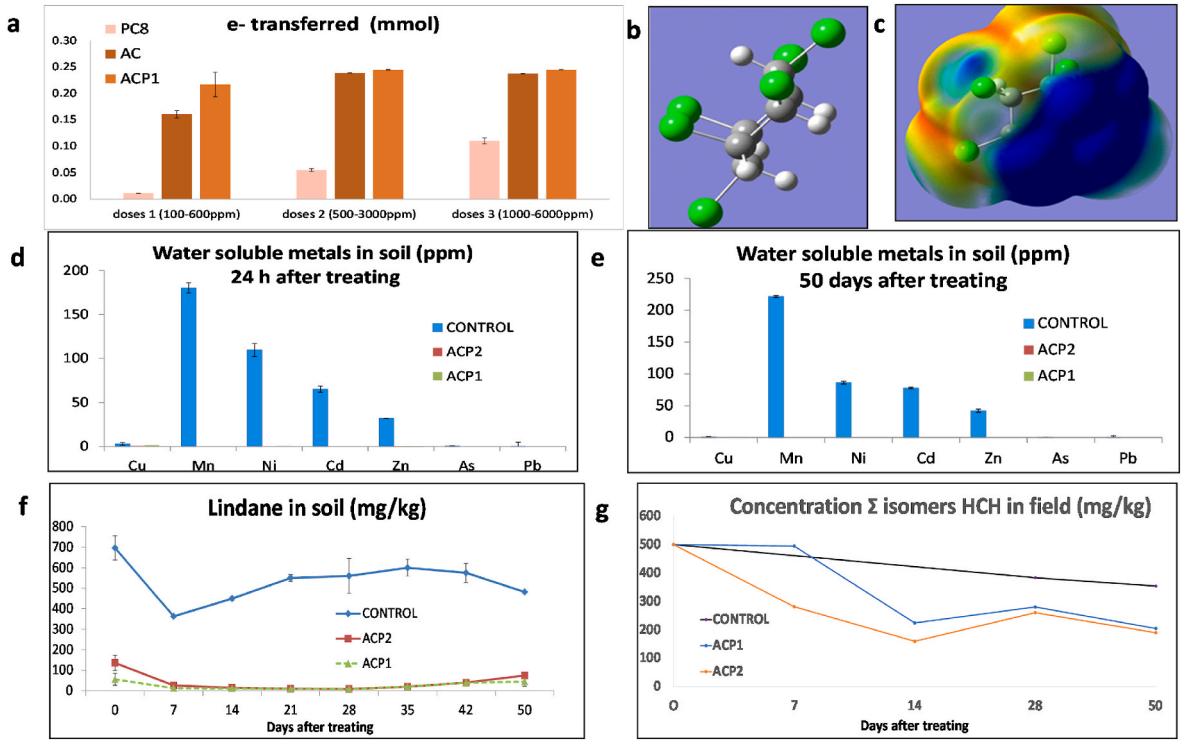

Fig. 5. Mechanism of action of ACP and efficiency in a real and artificial soil. **a.** Electron transfer capacity of ACP and its components at different doses. **b.** Optimized geometry of lindane (γ-isomer of hexachlorecyclohexane (HCH)) and **c.** Iso-surface MEP Map: blue, positive; red, negative. **d.** Soluble heavy metals remaining in an artificial soil after treating with two doses of ACP compared to untreated soil at 24 and **e.** 50 days after treating. **f.** Lindane remaining in an artificial soil after treating with two doses of ACP compared to untreated soil. **g.** Evolution of HCH in a real soil with ACP compared to the untreated soil.

a homogeneous distribution of lindane and heavy metals throughout the soil. When applying ACP to soil it is required to water to field capacity, as described in Methods, in order to supply the medium for the reaction of ACP with pollutants, as well as to provide the hydroxides to form the LDH from the PC8.

Fig. 5d shows that Mn, Ni, Cd and Zn were the principal metals extracted with water from the previously contaminated soil. The rest of the added metals were probably precipitated or adsorbed on different soil components such as clays or organic matter. As shown in Fig. 5d, both ACP formulations completely removed water-soluble metals from the soil within 24 h of application. This immobilization was stable over the time of the experiment (Fig. 5e).

Fig. 5f shows the evolution of lindane remaining in the soil, for the control and ACP treatments. This lindane fraction was extracted with hexane. Therefore, it includes both free and adsorbed lindane present in the soil. As can be seen, the two ACP treatments remove around 85% of the lindane after 24 h of application, and almost 100% of the lindane after 7 days of treatment. This shows a rapid, complete, and irreversible removal of a high lindane concentration (500 mg/kg) in the soil.

These results also indicate the ability of ACP to remove organic and inorganic contaminants. Likewise, they show that lindane degradation does not affect the ability of ACPs to immobilize the water-soluble fraction of heavy metals present in the soil, contrary to what has been suggested by other authors (Yin et al., 2007).

The mechanisms responsible for the ACP-mediated lindane elimination in the soil were studied in-depth, following the main byproducts generated during the process. Table 2 shows the main byproducts desorbed from soil mixed with ACP formulations. The main byproduct observed was 1, 2, 4-trichlorobenzene (the main byproduct of the dehydrohalogenation reaction), although dichlorobenzenes, benzene, and chlorophenols (byproducts of the dihaloelimination reaction) are also present. This is in line with the above-discussed results regarding the elimination of lindane in solution and supports dehydrohalogenation as the primary mechanism of lindane elimination with dihaloelimination as a complementary pathway of lindane degradation.

These results show the ability of ACP formulations to remove lindane in soil and immobilize heavy metal soil water-soluble fraction.

3.5. *Efficiency of ACP formulations to eliminate lindane in a highly contaminated soil*

A study was carried out in a soil in Bailín (Sabiñánigo, Spain). In this region of Spain there are landfills of lindane (Fig. 5g). Several 5 kg-samples of contaminated mud soil were taken from that location and treated with ACP formulations: ACP1 and ACP2, as described in Methods. The samples contained about 600 mg kg^{-1} of the sum of all the isomers of hexachlorocyclohexane (HCH). The applied doses of each treatment were 15% in the soil (Fig. 5g). In this case, heavy metals in the mud soil were negligible. The experimental design and methodology of the study are described in detail in Methods.

Fig. 5g shows the evolution of the sum of HCH isomers in mud soils treated with the two ACP formulations compared to untreated mud soil. The decrease of HCH in the soil with the treatments was apparent, reaching the maximum decrease at 14 days from the beginning of the application. The higher proportion of AC in ACP2 results in a more significant and faster elimination of HCH. The slight increase observed at 28 days may be due to variability in the soil trial. The HCH decrease represented 70% of the initial HCH content. A progressive decrease in HCH can be observed in the untreated sample, likely resulting from HCH volatilization. The extraction of HCH from each sample was carried out with hexane, thus revealing the total amount of HCH present in the mud-soil after the treatments. Therefore, the elimination of HCH results from its chemical and irreversible degradation by the action of ACP. The main limiting aspect of this study was obtaining homogeneous samples in which the mud soil and ACP are well mixed. However, this situation well represents the problems inherent in the field application of ACP. In fact, the HCH isomers were present in the contaminated mud soil as coarse particles that were difficult to grind. This fact may also explain the differences in efficacy between the artificial soil-level study and this natural soil-level study.

Table 3 shows the main byproducts present in the mud-soil at the end of the treatments. The high concentration of these compounds in the untreated soil indicates the natural degradation of HCH. In general terms, the sum of dichlorobenzenes, tetrachlorobenzenes and pentachlorobenzenes, together with chlorophenols, are decreased by ACP formulations. Likewise, the results show that a higher concentration of AC in ACP2 improves the efficiency of the treatment. It should be noted that the action of ACP removes not only HCH isomers but also other contaminants resulting from lindane degradation. In the case of trichlorobenzenes, especially 1,2,3-TCB, there is an increase in their concentration, probably related to the byproducts generated by the elimination of lindane as previously observed in studies in solution and soil at the laboratory level. In this sense, the byproducts found in the mud soil, mainly trichlorobenzenes and dichlorobenzenes, support the dehydrochlorination reaction and the reductive dihaloelimination as the

Table 2
Byproducts remaining in lindane-doped soil after treatments.

Byproducts remaining in soil (mg kg-1 dry basis)			
	CONTROL	ACP1	ACP2
Chlorides (1:5 p/v)	290	1300	1250
1,2,4-Trichlorobenzene	<0.015	>0.150 (1.14)	>0.150 (1.37)
1,2-Dichlorobenzene	<0.015	0.141	0.266
1,4-Dichlorobenzene	<0.015	0.146	>0.150 (0.287)
Benzene	<0.015	<0.015	0.017
Bromodichloromethane	002	0,3	005
Chlorobenzene	<0.015	0021	0056
Chlorodibromomethane	<0.015	0033	0051
Chloroform	0140	0070	0.112
Methylene Chloride	0.040	0.024	0.074
maximum sum BTEX	<0.090	<0.090	0092
Carbon tetrachloride	0.115	0039	0064
α-Hexachlorociclohexane	0.152	<0.100	<0.100
2,4-dichlorophenol	<0.400	<0.400	0.811
2,4,5 + 2,4,6-Trichlorophenol	<0.400	<0.400	0,94

Table 3
Byproducts remaining in highly lindane-contaminated soil after treatments.

Phenol	Byproducts in highly contaminated field			
	28 days after treating			
	Unities (dry basis)	**CONTROL**	**ACP1**	**ACP2**
	mg/kg ms	0.69	0.26	0.21
Chlorobenzenes				
Monochlorobenzenes	mg/kg ms	0.44	0.62	0.64
Sum of dichlorobenzenes	**mg/kg ms**	**170**	**900**	**780**
1,2-Dichlorobenzene	mg/kg ms	670	480	430
1,3-Dichlorobenzene	mg/kg ms	0.69	1,10	1,30
1,4-Dichlorobenzene	mg/kg ms	920	310	210
1,2,3-Trichlorobenzene	μg/kg ms	4500	7200	9200
1,2,4-Trichlorobenzene	μg/kg ms	32,000	22,000	28,000
1,3,5-Trichlorobenzene	μg/kg ms	<680	580	960
Sum of Trichlorobenzenes	**μg/kg ms**	**37,000**	**30,000**	**38,000**
1,2,4,5 + 1,2,3,5 Tetrachlorobenzene	μg/kg ms	15,000	18,000	17,000
1,2,3,4-Tetrachlorobenzene	μg/kg ms	24,000	18,000	15,000
Sum of Tetrachlorobenzenes	**μg/kg ms**	**39,000**	**36,000**	**32,000**
Pentachlorobenzenes	**μg/kg ms**	**3500**	**1300**	**920**
Hexachlorobenzenes	**μg/kg ms**	**<680**	**<280**	**<280**
Chlorophenols				
Sum of monochlorophenols	mg/kg ms	020	003	<0.03
Sum of dichlorophenols	mg/kg ms	0.51	0.17	0,05
Sum of trichlorophenols	mg/kg ms	140	0.94	0.26
Sum of tetrachlorophenols	mg/kg ms	005	0.19	0,08
Total Chlorophenols	mg/kg ms	220	130	0.41

main pathways involved in the mechanism responsible for the elimination of HCHby ACPformulations.

4. Conclusions

These results show the ability of this easy-to-produce and cost-effective new composite to remove lindane from highly contaminated soils. Likewise, the efficiency of the compound makes it a very valuable shock treatment for highly contaminated sites such as landfills that contain lindane residues to reduce the concentration of lindane to levels compatible with a second treatment. This second treatment might involve specific microorganisms capable of degrading the lindane and the resulting byproducts of lindane degradation. These effects are accompanied by the possibility of immobilizing heavy metals when they are present in soils with lindane or other organic contaminants.

The results also indicate that the ability of the new composite to remove lindane in soil and water solution is due to the synergistic action of its components. Thus, the combination of AC and PC8 allows the formation of microsites with basic local pH and a reducing atmosphere where lindane fixes and decomposes through two main elimination pathways: base-catalyzed dehydrochlorination and reductive dihaloelimination.

Author statement

Javier Erro Garcés: Conceptualization, Methodology, Investigation, Visualization, Writing – original draft. **José-Manuel Martínez-Pérez**: Investigation. **Maitane Guembe Contreras**: Resources, Project administration. **Raúl López Márquez**: Investigation, Validation. **José María García-Mina**: Conceptualization, Supervision, Formal analysis, Writing – review & editing.

Declaration of competing interest

The authors declare the following financial interests/personal relationships which may be considered as potential competing interests: JAVIER ERRO GARCES has patent COMPOSITE FOR THE SIMULTANEOUS AND IRREVERSIBLE REMOVAL OF INORGANIC AND ORGANIC CONTAMINANTS IN WATER OR SOIL pending to MAGNESITAS NAVARRA.

Data availability

No data was used for the research described in the article.

Acknowledgments

This research was funded by the Government of Navarra through the Projects 0011-1365-2016-000163.

Appendix A. Supplementary data

Supplementary data to this article can be found online at https://doi.org/10.1016/j.jenvman.2023.118476.

References

Al Juboury, M.F., Abdul-Hameed, H.M., 2020. Using of activated carbon derived from agriculture waste coating by layered double hydroxide for copper adsorption. In: International Conference on Environment.

Aldawsari, A.M., Alsohaimi, I., Hassan, H.M., Abdalla, Z.E., Hassan, I., Berber, M.R., 2021. Tailoring an efficient nanocomposite of activated carbon-layered double hydroxide for elimination of water-soluble dyes. J. Alloys Compd. 857, 157551. https://www.chemicalbook.com/SpectrumEN_7786-30-3_ir1.htm. (Accessed 26 May 2023).

Dorsey, A., 2005. Toxicological Profile for Alpha-, Beta-, Gamma, and Delta-hexachlorocyclohexane. Agency for Toxic Substances and Disease Registry, Atlanta, Georgia.

Fernández, J., Arjol, M.A., Cacho, C., 2013. POP-contaminated sites from HCH production in Sabiñánigo, Spain. Environ. Sci. Pollut. Res. 20 (4), 1937–1950.

Fu, R., Zeng, H., Lu, Y., 1993. The reducing property of activated carbon fibre and its application in the recovery of gold. Miner. Eng. 6 (7), 721–729.

Gao, Z., Sasaki, K., Qiu, X., 2018. Structural memory effect of Mg–Al and Zn–Al layered double hydroxides in the presence of different natural humic acids: process and mechanism. Langmuir 34 (19), 5386–5395.

García, M.A., Chimenos, J.M., Fernández, A.I., Miralles, L., Segarra, M., Espiell, F., 2004. Low-grade MgO used to stabilize heavy metals in highly contaminated soils. Chemosphere 56 (5), 481–491, 8.

Ismailov, A., Merilaita, N., Solismaa, S., Karhu, M., Levänen, E., 2020. Utilizing mixed-mineralogy ferroan magnesite tailings as the source of magnesium oxide in magnesium potassium phosphate cement. Construct. Build. Mater. 231, 117098.

Keppetipola, N.M., Dissanayake, M., Dissanayake, P., Karunarathne, B., Dourges, M.A., Talaga, D., et al., 2021. Graphite-type activated carbon from coconut shell: a natural source for eco-friendly non-volatile storage devices. RSC Adv. 11 (5), 2854–2865.

Kirisits, M.J., Snoeyink, V.L., Kruithof, J.C., 2000. The reduction of bromate by granular activated carbon. Water Res. 34 (17), 4250–4260.

Kumar, D., Pannu, R., 2018. Perspectives of lindane (γ-hexachlorocyclohexane) biodegradation from the environment: a review. Bioresour. Bioprocess. 5 (1), 1–18.

Li, S., Elliott, D.W., Spear, S.T., Ma, L., Zhang, W.X., 2011. Hexachlorocyclohexanes in the environment: mechanisms of dechlorination. Crit. Rev. Environ. Sci. Technol. 41 (19), 1747–1792.

Li, Y., Zhang, X., Shang, C., 2010. Effect of reductive property of activated carbon on total organic halogen analysis. Environ. Sci. Technol. 44 (6), 2105–2111.

Liu, Y., Liu, X., Dong, W., Zhang, L., Kong, Q., Wang, W., 2017. Efficient adsorption of sulfamethazine onto modified activated carbon: a plausible adsorption mechanism. Sci. Rep. 7 (1), 1–12.

Ma, J., Yang, Y., Jiang, X., Xie, Z., Li, X., Chen, C., Chen, H., 2018. Impacts of inorganic anions and natural organic matter on thermally activated persulfate oxidation of BTEX in water. Chemosphere 190, 296–306.

Madaj, R., Sobiecka, E., Kalinowska, H., 2018. Lindane, kepone and pentachlorobenzene: chloropesticides banned by Stockholm convention. Int. J. Environ. Sci. Technol. 15 (2), 471–480.

Manohara, G.V., Prasanna, S.V., Kamath, P.V., 2011. Structure and composition of the layered double hydroxides of Mg and Fe: implications for anion-exchange reactions. Eur. J. Inorg. Chem. 2624–2630.

Murray, J.S., Politzer, P., 2017. Molecular electrostatic potentials and non-covalent interactions. Wiley Interdiscip. Rev. Comput. Mol. Sci. 7 (6), e1326.

Pramanik, A., Das, S., Sarkar, P., Appavoo, S., 2018. Adsorbent Comprising Layered Double Hydroxide and Activated Carbon. WO 2018046286A1.

Ruowen, F., Hanmin, Z., Yun, L., 1993. The reduction property of activated carbon fibers. Carbon 31 (7), 1089–1094.

Tang, Z., Qiu, Z., Lu, S., Shi, X., 2020. Functionalized layered double hydroxide applied to heavy metal ions absorption: a review. Nanotechnol. Rev. 9 (1), 800–819.

Tao, Q., Zhang, Y., Zhang, X., Yuan, P., He, H., 2006. Synthesis and characterization of layered double hydroxides with a high aspect ratio. J. Solid State Chem. 179 (3), 708–715.

Usman, M., Tascone, O., Faure, P., Hanna, K., 2014. Chemical oxidation of hexachlorocyclohexanes (HCHs) in contaminated soils. Science of the Total Environment 476, 434–439.

Vera, J., Correia-Sá, L., Paíga, P., Bragança, I., Fernandes Virgínia, C., Domingues Valentina, F., Delerue-Matos, C., 2013. QuEChERS and soil analysis. An Overview Sample Preparation 1–54.

Vijgen, J., Abhilash, P.C., Li, Y.F., Lal, R., Forter, M., Torres, et al., 2011. Hexachlorocyclohexane (HCH) as new Stockholm Convention POPs—a global perspective on the management of Lindane and its waste isomers. Environ. Sci. Pollut. Res. 18 (2), 152–162.

Vithanage, M., Ashiq, A., Ramanayaka, S., Bhatnagar, A., 2020. Implications of layered double hydroxides assembled biochar composite in adsorptive removal of contaminants: current status and future perspectives. Sci. Total Environ. 737, 139718.

Xin, D., Xian, M., Chiu, P.C., 2018. Chemical methods for determining the electron storage capacity of black carbon. MethodsX (5), 1515–1520.

Yin, C.Y., Aroua, M.K., Daud, W.M.A.W., 2007. Review of modifications of activated carbon for enhancing contaminant uptakes from aqueous solutions. Sep. Purf. Technol. 52 (3), 403–415.

Zhang, C., Zhang, D., Li, Z., Akatsuka, T., Yang, S., Suzuki, D., Katayama, A., 2014. Insoluble Fe-humic acid complex as a solid-phase electron mediator for microbial reductive dechlorination. Environ. Sci. Technol. 48 (11), 6318–6325.

Zhang, F., Song, Y., Song, S., Zhang, R., Hou, W., 2015. Synthesis of magnetite–graphene oxide-layered double hydroxide composites and applications for the removal of Pb (II) and 2, 4-dichlorophenoxyacetic acid from aqueous solutions. ACS Appl. Mater. Interfaces 7 (13), 7251–7263.

Zhang, W., Lin, Z., Pang, S., Bhatt, P., Chen, S., 2020. Insights into the biodegradation of lindane (γ-hexachlorocyclohexane) using a microbial system. Front. Microbiol. 11, 522.

Zubair, M., Ihsanullah, I., Aziz, H.A., Ahmad, M.A., Al-Harthi, M.A., 2021. Sustainable wastewater treatment by biochar/layered double hydroxide composites: progress, challenges, and outlook. Bioresour. Technol. 319, 124128.